

Michael K. Sharp

Department of Civil Engineering, Rensselaer Polytechnic Institute, Troy, NY 12180, USA and Waterways Experiment Station, Vicksburg, MS 39180, USA.

Ricardo Dobry

Department of Civil Engineering, Rensselaer Polytechnic Institute, Troy, NY 12180, USA.

Ryan Phillips

C-CORE, Memorial University, St John's, Newfoundland, Canada, A1B 3X5

ABSTRACT: This paper reports research currently being conducted on the correlation of permanent lateral ground deformation (D_H) due to earthquake-induced lateral spreading caused by liquefaction of saturated sand, with static cone penetration (CPT) point resistance. Both lateral spreading tests with in-flight shaking and in-flight CPT tests are done at the Rensselaer Polytechnic Institute (RPI) centrifuge in Troy, N.Y. D_H measurements are being directly correlated with the CPT in centrifuge model tests for various sand relative densities and degrees of preshaking. These correlations will provide the basis for CPT-based charts to predict D_H in the field. These charts are also expected to provide threshold combinations of CPT value, soil depth, ground slope, and strong motion input for which D_H is small and can be neglected even if the soil liquefies, due to its dilatant shear stress-strain response.

1 INTRODUCTION

Liquefaction of loose, water-saturated sands and other granular soils due to earthquake shaking is a major cause of damage to and destruction of constructed facilities. One of the major liquefaction induced types of ground failure is lateral spreading of mildly sloping ground. A 2-year research effort focusing on evaluation of permanent lateral ground deformation (D_H) due to lateral spreading, using the in situ static cone penetration testing (CPT) technique is being conducted at Rensselaer Polytechnic Institute (RPI), Troy, NY. In this investigation, lateral spreading D_H measurements are directly correlated with the CPT in centrifuge model tests for various sand relative densities and degrees of preshaking. These correlations, after proper verification against the available empirical and case history information related to both CPT and D_H in the field are expected to provide the basis for CPT-based charts to predict D_H in the field for given ground slope, soil conditions, and strong motion input. Also, these charts should provide further clarification of the threshold combinations of CPT value, soil depth, ground slope, and strong motion input for which D_H becomes small and can be

neglected even if the soil liquefies, due to its dilatant shear stress-strain response.

This research employs physical prototype modeling using the centrifuge facilities at RPI and the development of a miniature CPT and containers appropriate for centrifuge testing. Several investigators have also shown promising results of modeling the CPT in sand in the centrifuge, with results reported by Phillips and Valsangkar (1987), Corte et al. (1991), and Renzi et al. (1994). The results reported by Corte, and Renzi have also shown that a CPT profile conducted in the centrifuge can be used to predict tip resistance, q_c , in the field. Extensive work at RPI using a laminar box container inclined to the horizontal and shaken at the base have demonstrated the usefulness of centrifuge simulation of the lateral spreading phenomenon (Dobry et al., 1995; Taboada, 1995).

2 CENTRIFUGE MODELING OF LATERAL SPREADING

Figure 1 shows the inclined RPI laminar box container used by Taboada (1995) to model lateral spreading in the centrifuge, while Fig. 2 includes some results obtained in three duplicate tests performed at RPI and California Institute of Technology. In these experiments the saturated,

loose sand layer is inclined a few degrees to the horizontal to simulate an infinite sloping deposit, and is excited in-flight at the base of the container by a simulated earthquake acceleration time history (Fig. 1). This earthquake excitation causes the soil to liquefy, and downslope permanent lateral displacements D_H develop in the liquefied soil by the combined effect of static and dynamic shear stresses (Fig. 2).

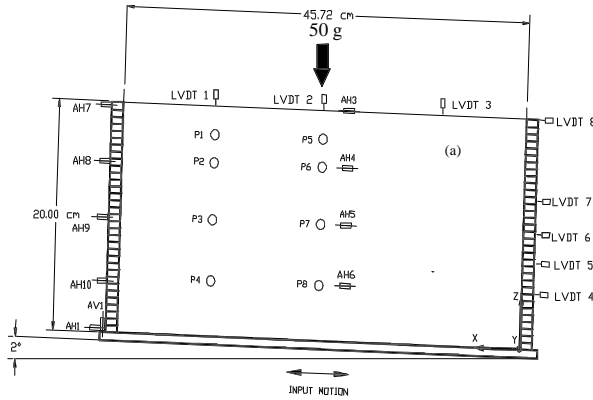


Figure 1. RPI laminar box and model setup (Taboada, 1995).

Acceleration (A), pore pressure (P) and vertical and horizontal displacement (LVDT) transducers (Fig. 1) measure the corresponding parameters during and after shaking. In particular, the permanent lateral displacement profiles of Fig. 2 were measured by transducers LVDT4, LVDT5, LVDT6, LVDT7, and LVDT8 mounted on the rings of the flexible-wall laminar box container of Fig.1. The results of Fig. 2 correspond to a test on water-saturated fine Nevada sand, prepared at a relative density of $D_r = 40$ to 45%, spun at 50 g centrifugal acceleration (that is, the 20 cm sand layer of Fig. 1 simulates a 10 m layer in the field), and excited at the base by a maximum prototype earthquake acceleration of about 0.2 g (Taboada, 1995). Values of surface permanent lateral ground displacement of about $D_H = 0.5$ m were measured in these tests (Fig. 2). This same lateral spreading modeling technology will be used by the authors in their research aimed at correlating CPT and D_H .

3 DEVELOPMENT OF MINIATURE CPT SYSTEM

The system consists of a miniature CPT appropriate for testing in the centrifuge, with three miniature cones used in conjunction with the soil model container. The in-flight CPT (Fig. 3) is an electric chain driven system capable of penetrating into the

soil model a distance of 1 m. The soil model container is cylindrical with a diameter of 50 cm and height in excess of 1 m. It is possible to model a soil deposit with a maximum field thickness of approximately 20 m. The miniature cones have diameters of 4, 8, and 12 mm, respectively. The use of three different cones was planned such that varying centrifugal accelerations could be tested while still maintaining the proper scaling relationship with the standard field CPT. That is, the 4 mm cone is being used at a centrifuge acceleration of 9g, the 8 mm cone at 4.5g, and the 12 mm cone at 3g, with all of them modeling the prototype CPT in the field at 1g having the standard diameter of 36 mm. In this way, each one of the cones serves as a 'model of the models' for the others, thus increasing the confidence of the results. Some of these CPT tests will be repeated later in the laminar box of Fig. 1 to be used in the lateral spreading experiments, to verify that the CPT results in the system of Fig. 3 are valid for the sand in the laminar box.

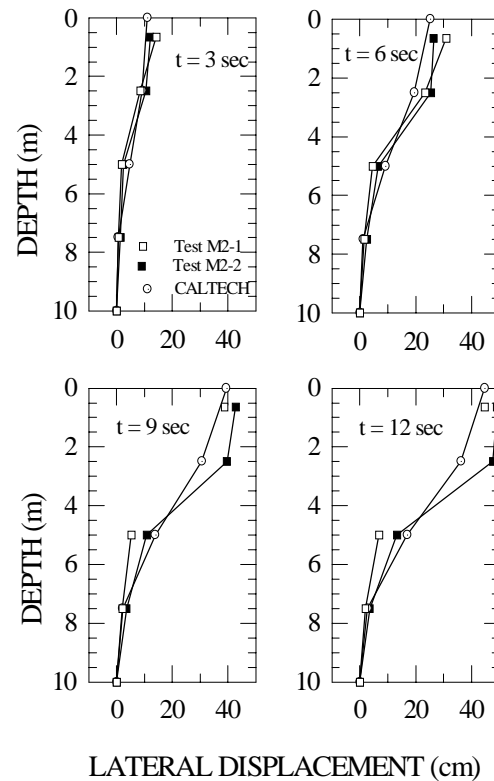


Figure 2. Lateral displacement profiles at various times during shaking from tests at RPI and CALTECH (Taboada, 1995).

3.1 Container Boundary Effects

Container size and boundary conditions can affect CPT measurements. Several researchers have investigated the influence of boundary conditions on

CPT data and have established a diameter ratio, R_d , defined as the ratio of the chamber diameter to cone diameter. Parkin and Lunne (1982) report results of an extensive series of tests to investigate boundary effects in flexible walled chamber tests. These results indicate that the side boundary effects depend on the relative density of the sand. For a loose sand with relative density on the order of 30%, the side boundary effects are negligible. For a dense sand the chamber diameter must be at least 50 times the diameter of the cone to eliminate the effect of the side boundary on cone resistance. Parkin and Lunne also report the results of work in a rigid walled chamber. The range of diameter ratios in that study was 28 to 39.7.

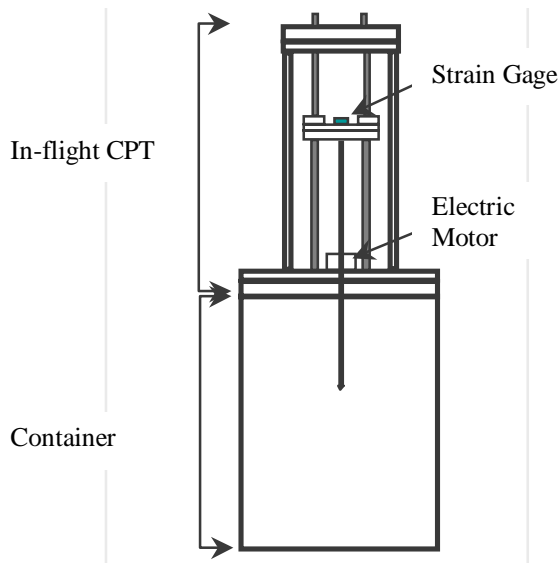


Figure 3. Schematic of In-flight CPT system.

These results indicate that for rigid walled chambers the side boundary effects are not significant when the diameter ratio is greater than 28. In tests reported by Gui (Renzi et al., 1994), specimens prepared at medium and high densities (1532 kg/m^3 and 1663 kg/m^3) showed no apparent increase in q_c for tests done at a ratio $R_d = 42$ compared to $R_d = 85$. These tests were performed in a cylindrical container. Bagge (Renzi et al., 1994) also reported results in a cylindrical container performed on tests at soil high density (1627 kg/m^3) and found that there was no apparent increase in q_c for tests executed at $R_d = 11$ as compared to the reference test at $R_d = 22$. For the penetrometers and container developed at the RPI centrifuge, the minimum R_d values for the 4, 8 and 12 mm cones for pushes located at the center of the container are 125, 62.5, and 41.6 respectively. These values are larger than those reported in the literature and should

assure that no boundary effects will occur for pushes made at the center of the container. For these pushes made in the center of the container, the failure mechanism is as described for a simple footing on infinite ground. In addition to the center of the container, pushes are also performed in the RPI investigation along two concentric circles, with the outer circle being 10 cm from the container's edge. Pushes made close to the boundary would allow the failure mechanism to develop freely on the side of the probe away from the boundary but will be constrained on the side toward the boundary. In testing similar to this, Phillips and Valsangkar (1987) reported that for rigid walled tests on sand with a $D_r = 87\%$, side wall boundary effects are negligible even when the probe is located at a distance from the wall corresponding to $R_d = 5$. Using 10 cm as the distance to the wall gives R_d values of 25, 12.5, and 8.3 for the three cones used at RPI. As shown later by the preliminary results of in-flight cone penetration at RPI, these cone diameters and push locations showed no effect from the side-wall boundaries, as expected.

With respect to the bottom boundary effect, Phillips and Valsangkar (1987) reported that for a 10 mm cone, the bottom boundary effects are seen starting at a vertical distance of 10 to 12 cone diameters. In the case of the cones used in this experiment, the expected distance of bottom influence would be 48 mm for the 4 mm cone, 96 mm for the 8 mm cone, and 144 mm for the 12 mm cone. The tests at RPI reveal a bottom influence at vertical distances from the bottom consistent with these and others reported in the literature.

3.2 Rate of Penetration Effects

The prototype standard penetration rate for the CPT in the field is 2 cm/sec; for the in-flight tests being conducted at the RPI centrifuge the model penetration rate is 1 mm/sec. Phillips and Valsangkar (1987) reported results of centrifuge tests in sand performed at penetration rates of 2-4 mm/sec with no noticeable difference in results. They also reported no difference in results for tests performed at a rate of 10 mm/sec. Work done by Corte et al. (1991), revealed that tests done in fine sand did not show a noticeable influence of rate of penetration in the range from 0.5 mm/sec to 10 mm/sec, and that the penetration test appears to be a drained event in saturated sand. The rate of 1 mm/sec for the tests being conducted at RPI is believed to be consistent with prototype measurements, and also to be slow

enough so as to assure drained conditions when a saturated sand model is tested.

3.3 Grain Size Effects

The soil selected for these experiments is Nevada sand, having geotechnical properties as previously measured by Arulmoli et al. (1992). This is the same sand that will be used for the lateral spreading experiments in the laminar box. The specific gravity of Nevada sand was determined to be 2.67 and the maximum and minimum unit weights were found to be 17.33 kN/m^3 (minimum void ratio = 0.511) and 13.87 kN/m^3 (maximum void ratio = 0.887), respectively. The grain size ranges from 0.1 to 0.25 mm and the soil classifies as a fine sand. Laue (Renzi et al., 1994) reported that soil particle size does not affect the results for a ratio d_c / d_{50} in the range of 90 to 50, where d_c is the model cone diameter. For Nevada sand, $d_{50} = 0.13 \text{ mm}$, which gives $d_{4\text{mm}} / d_{50} = 30.7$, $d_{8\text{mm}} / d_{50} = 61.5$, and $d_{12\text{mm}} / d_{50} = 92$. Ovesen (1981) reported that significant size effects are observed when d_c / d_{50} is less than 30. This would imply that utilizing fine sand gives a minimum cone diameter requirement on the order of 6 mm. The value of 30.7 for the 4 mm cone of this test may be on the edge of values that would start producing grain size effects. However, no grain size effects were observed in the data for the 4 mm cone, as indicated by the excellent ‘model-of-the-model’ comparisons with the other cones.

4 CPT CENTRIFUGE TESTS PERFORMED

Centrifuge results reported in this paper are from in-flight CPT on several relative densities and dry and saturated Nevada sand models. The sand was placed dry using the sand raining technique.

Initial tests on a model prepared at a $D_r=75\%$ revealed results as shown in Fig. 4. The change in slope at a vertical effective stress of 20 kPa is attributed to arching in the container of Fig. 3. The data shown in Fig. 4 was collected with the 8 mm cone at 4.5g on a model prepared dry at $D_r=75\%$. Subsequent tests with the other cones and models prepared both dry and saturated showed very similar results. This problem was overcome by greasing the container and lining it with a latex membrane. The final combination of grease and membrane that proved most effective at eliminating the arching effect was a non-petroleum lubricant and a thin (0.02 mm) latex membrane.

In-flight CPT tests were performed on five models with nine to twelve cone penetrometer

probes per model. A typical model was tested with each of the three probes (4, 8, and 12 mm) and three to four tests per probe. The tests were conducted by starting at the lowest g level, 12 mm at 3g, and finishing at the highest g level, 4 mm at 9g. The models tested were as follows; $D_r=75\%$ dry, $D_r=75\%$ saturated, $D_r=65\%$ dry, $D_r=45\%$ dry and $D_r=45\%$ saturated.

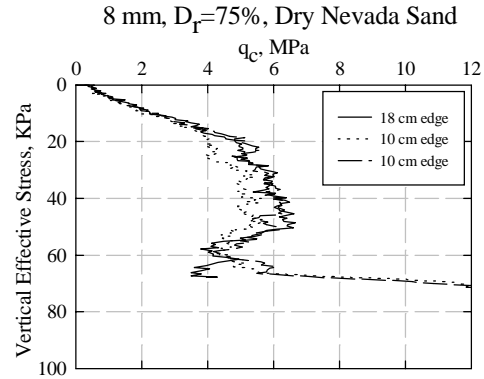


Figure 4. Arching effect on in-flight CPT data.

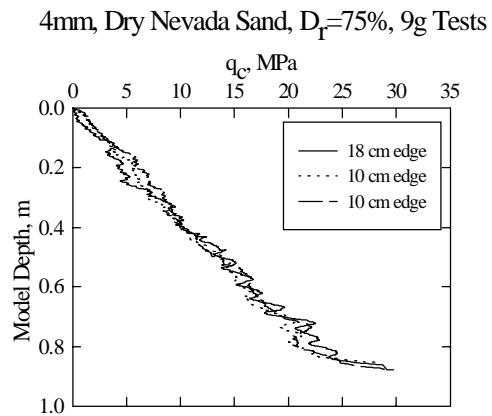


Figure 5. Container boundary effects of In-flight CPT data.

5 TESTS RESULTS AND DISCUSSION

Verification that data collected with the CPT system had no effects from the boundary is presented in Fig. 5. The results shown are for one push located 18 cm from the container boundary edge and two pushes located 10 cm from the boundary edge. The probes are also located 10 cm from each other. The data indicate excellent agreement between pushes, verifying that there are no boundary effects or ‘cone to cone’ proximity effects. The results shown are for a dry model, but similar data were also obtained in saturated models. It is also of interest to note that the arching effect clearly shown by the data in Fig. 4

has been almost entirely eliminated. This conclusion was also confirmed by the rest of the data.

Results of the ‘model of the models’ are shown in Figs. 6-8. Pushes were made with the 12 mm cone at 3g, 8 mm cone at 4.5g, and 4 mm cone at 9g. The particular parameters for each test are given in the following discussion. The agreement is excellent for all data shown.

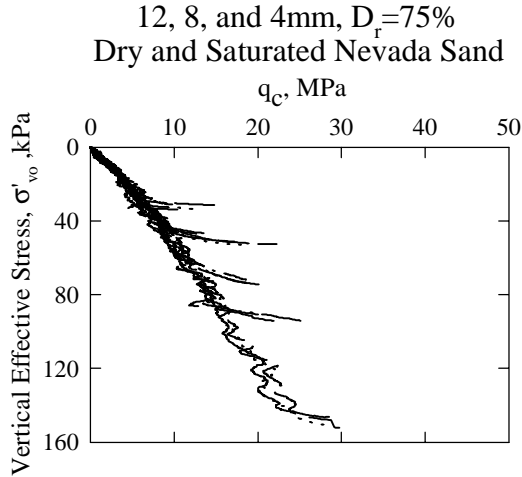


Figure 6. Results from $D_r=75\%$ tests, dry and saturated sand.

The measurements from all dry and saturated models prepared at $D_r=75\%$, and using the three probe sizes, are presented in Fig. 6 in prototype scale. The agreement is excellent, confirming again the ‘model of the models’ concept, as well as the agreement between dry versus saturated models at the same effective vertical stress, σ'_{vo} . One useful consequence of this agreement is that the plot of q_c versus σ'_{vo} in Fig. 6 can be used in a fully submerged deposit to a depth of about 20 m, despite the fact that the q_c measurements in the fully saturated sand models reached only to about 10 m prototype.

Results from the model prepared at $D_r=65\%$ are shown in Fig. 7. The data are from a dry model only with pushes made using all three cones. The agreement between the different pushes is very good.

Results for the models prepared at $D_r=45\%$ are shown in Fig. 8. The data are from a dry and a saturated model, with pushes made using all three cones. Here again the data agreement is excellent between the different probes and between the dry and saturated sand.

Utilizing the plots for the data collected from the three different relative densities (75%, 65%, and 45%), the data should fit an equation of the form, $q_c = q_{c1}(\sigma'_{vo})^c$. In this equation σ'_{vo} = the vertical effective stress in kPa, q_c = the tip resistance in kPa,

q_{c1} = normalized tip resistance in kPa, and c is the stress exponent. The parameters q_{c1} and c depend on the relative density of the soil and from the in-flight CPT tests of this experiment, the values are shown in Fig. 9. These values and trends with σ'_{vo} are in excellent agreement with those reported by Olsen (1994) and others.

Combining the results from the in-flight CPT data as summarized in Fig. 10(a) with the expected liquefaction and lateral spreading results sketched in Fig. 10(b), the results sketched in Fig. 10(c) are to be obtained. This is a plot of liquefaction-induced lateral spreading versus CPT. Fig. 10(c) is a conceptual plot of the expected prediction charts to be developed in this research.

12, 8 and 4mm, Dry Nevada Sand, $D_r=65\%$

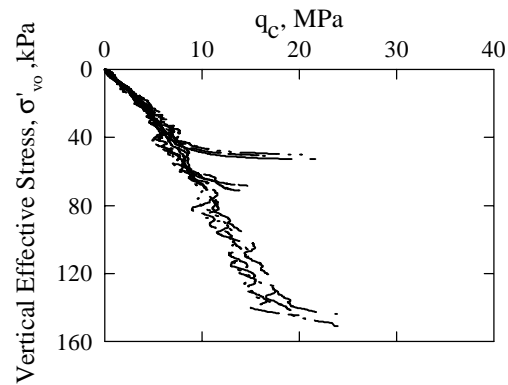


Figure 7. Results from $D_r=65\%$ tests dry model.

12, 8, and 4 mm, $D_r=45\%$
Dry and Saturated Nevada Sand

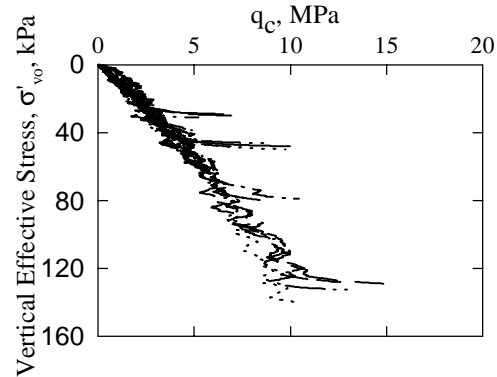


Figure 8. Results from $D_r=45\%$ tests, dry and saturated sand.

DISCUSSION AND CONCLUSIONS

Several conclusions can be drawn from testing of the RPI in-flight CPT system. The boundary effects are negligible, the ‘model of the models’ concept works very well, there is good correlation between dry and saturated models,

arching was almost entirely eliminated from the data, and the CPT is a very useful tool for characterizing different relative densities in soil. The CPT data presented in this paper are reasonably consistent with that reported by other researchers. A concept has been formulated to develop prediction charts from the CPT data with liquefaction-induced lateral spreading centrifuge tests.

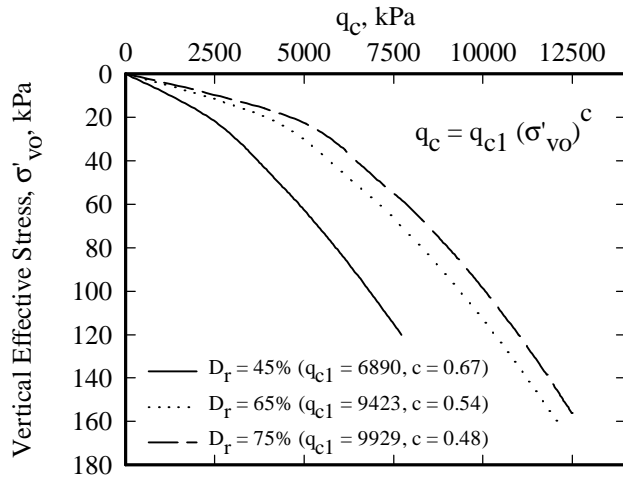


Figure 9. Plot of q_c versus σ'_{vo} with curves corresponding to various D_r , and showing descriptive parameter q_{c1} .

Ongoing research in this project will focus on obtaining additional lateral spreading data from centrifuge tests such as done by Taboada (1995) and illustrated by Figs. 1-2, and correlating with the CPT data presented in this paper. Important parameters that will be considered in both the centrifuge lateral spreading tests, and in additional CPT model tests in the containers of Figs. 1 and 3, are: sand relative density, over consolidation ratio, soil permeability, earthquake input acceleration and duration, and effect of preshaking.

ACKNOWLEDGEMENTS

This research was funded by the United States Geological Survey and the U.S. Army Engineer,

Waterways Experiment Station. This support is greatly appreciated.

REFERENCES

- Arumoli, K., K.K. Muraleetharan, M.M. Hossain and L.S. Fruth (1992), "Verification of Liquefaction Analysis by Centrifuge Studies Laboratory Testing Program Soil Data Report," Report from The Earth Technology Corporation, Irvine, California.
- Corte, J.F., J. Garnier, L.M. Cottineau & G. Rault, (1991). "Determination of Model Soil Properties in the Centrifuge," Proc. of Int. Conf. Centrifuge 1991, Boulder, CO, 13-14 June, pp. 607-614.
- Dobry, R., V. Taboada, and L. Liu (1995). "Centrifuge modeling of liquefaction effects during earthquakes," Proc. First Intl. Conf. on Earthquake Geotechnical Engineering, Tokyo, Japan, November, Vol. 3.
- Olsen, R.S. (1994). "Normalization and Prediction of Geotechnical Properties Using the Cone Penetrometer Test (CPT)", Technical Report GL-94-29, U.S. Army Waterways Experiment Station.
- Ovesen, N.K., (1981). "Centrifuge tests of the uplift capacity of anchors", Proc. 10th International Conf. on SMFE, Stockholm, Sweden, Vol. 1, pp. 717-722.
- Parkin, A. K. and Lunne, T. (1982). "Boundary Effects in the Laboratory Calibration of a Cone Penetrometer in Sand," Proceedings of the Second European symposium on Penetration Testing, ESOPT II, Amsterdam, May 1982. Vol. 2, pp. 761-768.
- Phillips, R. and A. J. Valsangkar, (1987). "An Experimental Investigation of Factors Affecting Penetration Resistance in Granular Soils in Centrifuge Modeling," Report CUED/D-Soils TR 210, Cambridge.
- Renzi, R., J.F. Corte, G. Bagge, M. Gui, J. Laue, (1994). "Cone Penetration Tests in the Centrifuge: Experience of Five Laboratories," Proc. of International Conference Centrifuge 94, Singapore, 31 August-2 September, pp. 77-82.
- Taboada, V.M. (1995). "Centrifuge Modeling of Earthquake-Induced Lateral Spreading in Sand Using a Laminar Box", PhD Thesis, Rensselaer Polytechnic Institute, Troy, NY.

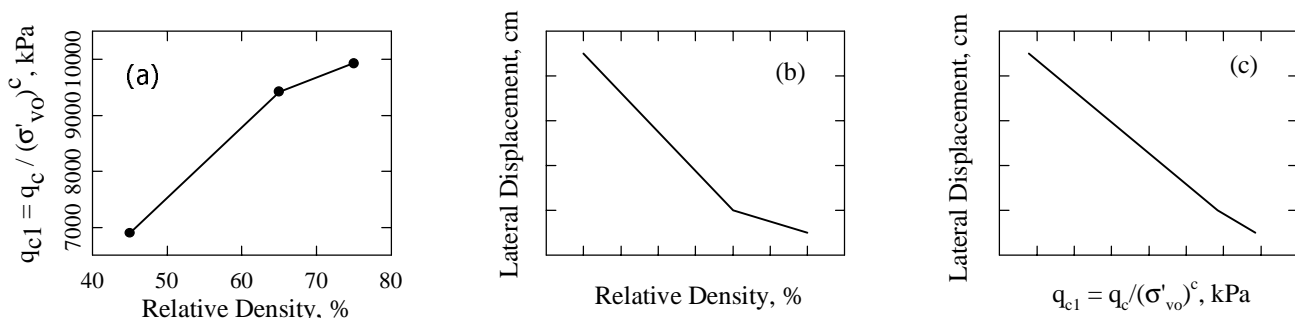


Figure 10. (a) actual plot of D_r versus q_{c1} determined from in-flight CPT test, (b) conceptual plot of D_H versus D_r from liquefaction-induced lateral spreading tests, (c) conceptual plot of D_H versus q_{c1} .